Structure, Volume *30*

Supplemental Information

Structural insights into the binding of SARS-CoV-2, SARS-CoV, and hCoV-NL63 spike receptor-binding domain to horse ACE2

Jun Lan, Peng Chen, Weiming Liu, Wenlin Ren, Linqi Zhang, Qiang Ding, Qi Zhang, Xinquan Wang, and Jiwan Ge

Structural insights into the binding of SARS-CoV-2, SARS-CoV and hCoV-NL63 spike receptor-binding domain to horse ACE2

Jun Lan[1,#], Peng Chen[2,#], Weiming Liu[5,#], Wenlin Ren[3], Linqi Zhang[2], Qiang Ding[3], Qi Zhang[2,*], Xinquan Wang[1,*], Jiwan Ge[1,4,6,*]

[1]The Ministry of Education Key Laboratory of Protein Science, Beijing Advanced Innovation Center for Structural Biology, Beijing Frontier Research Center for Biological Structure, School of Life Sciences, Tsinghua University, Beijing, China

[2]Comprehensive AIDS Research Center, Beijing Advanced Innovation Center for Structural Biology, School of Medicine and Vanke School of Public Health, Tsinghua University, Beijing, China

[3]Center for Infectious Disease Research, School of Medicine, Tsinghua University, Beijing, China; Beijing Advanced Innovation Center for Structural Biology, Tsinghua University, Beijing, China.

[4]Tsinghua-Peking Center for Life Sciences, Beijing, China

[5]Department of Critical Care Medicine, Beijing Boai Hospital, China Rehabilitation Research Centre; No 10. Jiaomen Beilu, Fengtai District, Beijing, 100068, China

[6]Lead contact

[#]Equal contribution

[#]Correspondence: zhangqi2013@mails.tsinghua.edu.cn (Q.Z.)

xinquanwang@mail.tsinghua.edu.cn (X.W.)

gejw@mail.tsinghua.edu.cn (J.G.)

Supplementary Table 1 Data collection and refinement statistics, related to Figure 2.

	SARS-CoV-2 RBD/eACE2	SARS-CoV RBD/eACE2	hCoV-NL63 RBD/eACE2
Data Collection			
Resolution range (Å)	50-2.895(2.998-2.895)	50-2.655(2.75-2.655)	50-3.193(3.307-3.193)
Space group	I 4_1 2 2	P 2_1 2_1 2_1	P 6_1 2 2
Unit cell dimensions			
a, b, c (Å)	196.173,196.173,144.36	57.963,126.314,171.637	112.905,112.905,328.924
α, β, γ (°)	90,90,90	90,90,90	90,90,120
Unique reflections	30247(2521)	37045(3573)	21422(2019)
Completeness (%)	95.46(81.06)	99.30(97.51)	98.76(97.25)
I/sigma	10.1(1.6)	16.8(1.5)	15.6(3.6)
redundancy	16.9(14.7)	8.9(7.6)	27.4(25.9)
rmerge	0.302(1.162)	0.147(1.333)	0.459(2.127)
Rpim	0.071(0.272)	0.049(0.464)	0.083(0.383)
CC1/2	0.986(0.807)	0.994(0.706)	0.978(0.869)
Wilson B-factor ($Å^2$)	47.67	58.56	64.08
Structure refinement			
Resolution	46.73-2.895	17.95-2.655	33.71-3.193
R_{work}/R_{free} (%)	0.2450/0.2656	0.2318/0.2546	0.2591/0.2800
No.atoms			
Protein	6404	6392	5876
Ligands	70	57	77
Protein residues	795	790	732
B-factors ($Å^2$)			
Protein	51.74	61.78	62.02
Ligands	59.02	49.18	98.12
RMSD			
Bonds length (Å)	0.012	0.011	0.013
Bonds angles (°)	1.59	1.37	1.93
Ramachandran plot			
Favored (%)	94.66	95.16	95.01
Allowed (%)	5.08	4.59	4.85
Outliers (%)	0.25	0.25	0.14

Supplementary Figure 1

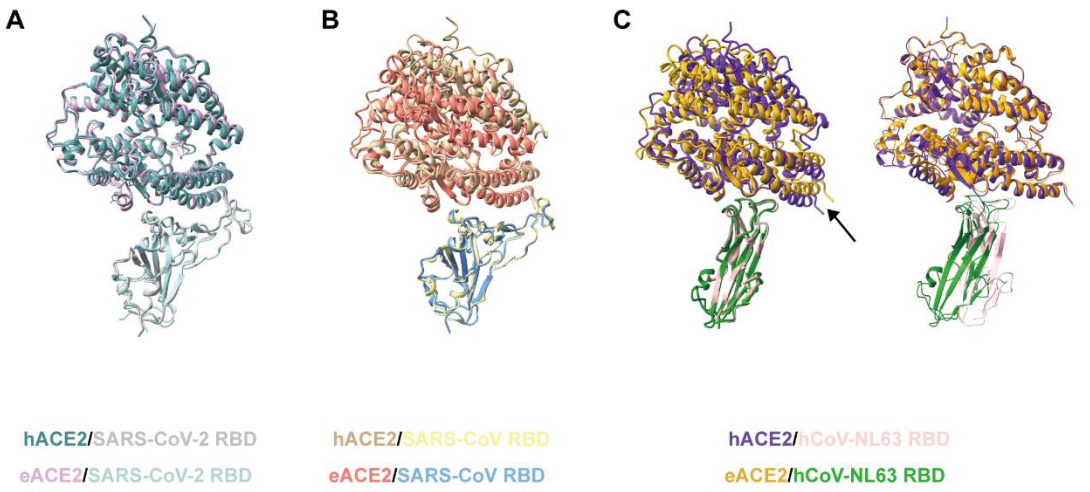

Supplementary Figure 1 Structural alignment of horse ACE2/RBDs with human ACE2/RBDs, related to Figure 3. Alignment was performed according to each RBD. (**A**) eACE2/SARS-CoV-2 RBD vs. hACE2/SARS-CoV-2 RBD. (**B**) eACE2/SARS-CoV RBD vs. hACE2/SARS-CoV RBD. (**C**) eACE2/hCoV-NL63 RBD vs. hACE2/hCoV-NL63 RBD. The arrow points to the difference in the N terminal helix. Left: alignment according to RBD; right: alignment according to ACE2.

Supplementary Table 2 Contact residues at the binding interfaces of RBDs and ACE2 orthologs (a distance cut-off 4 Å), **related to Figure 3**.

Human ACE2	SARS-CoV-2	SARS-CoV	hCoV-NL63	Horse ACE2	SARS-CoV-2	SARS-CoV	hCoV-NL63
Q24	A475, N487	N473		L24	A475, G476, N487	P462, N473	
T27	F456, A475, Y489	L443, Y475		T27	F456, Y489	L443, P462, Y475	
F28	Y489	Y475		F28	Y489	Y475	
D30	K417, F456		S496	E30	K417, F456	Y442, L443	
K31	Y489, Q493	Y442, Y475		K31	L455, F456, Q493	Y442, Y475	
N33			S496	N33			
H34	Y453, L455, Q493	Y440, N479	G494, G495, S496, H503	S34	Y453, L455, Q493	N479	
E35	Q493			E35	Q493		
E37	Y505	Y491	C497, Y498	E37	Y505	Y491	G495, S496
D38	Y449	Y436		E38	Y449, G496, Q498	Y436, G482	
Y41	Q498, T500, N501	Y484, T486, T487	G534, S535, P536	H41	N501	Y484	G534, S535
Q42	G446, Y449, Q498	Y436, Y484		Q42	G446, Y449, Q498	Y436, Y484	
L45		Y484, T486		L45	Q498	Y484	
L79	F486	L472		L79			
M82	F486	L472		T82	F486		
Y83	F486, N487, Y489	N473, Y475		Y83	F486, N487, Y489	N473, Y475	
P321			H586	P321			
N322			H586	N322			H586
M323				M323			H586
T324			S540, H586	T324			S540, W585, H586
Q325		R426, I489	P536, S540	Q325			S539
G326			P536	G326			P536
E329		R426		E329			
N330	T500	T486	P536	N330	T500	T486	P536
K353	G496, N501, G502, Y505	G482, T487, G488, Y491	Y498, S535, G537	K353	G496, Q498, N501, G502, Y505	G482, Y484, T487, G488, Y491	Y498, S535, G537
G354	G502, Y505	G488, Y491	Y498, S535, G537	G354	G502	G488, Y491	G537, W585
D355	T500	T486, G488	P536	D355	T500	T486	P536

F356			W585	F356			W585
R357	T500	T486		R357	T500	T486	P536
A386				A386			C497
A387			C500	V387			C497
R393	Y505		C497	R393	Y505		S496

Supplementary Figure 2

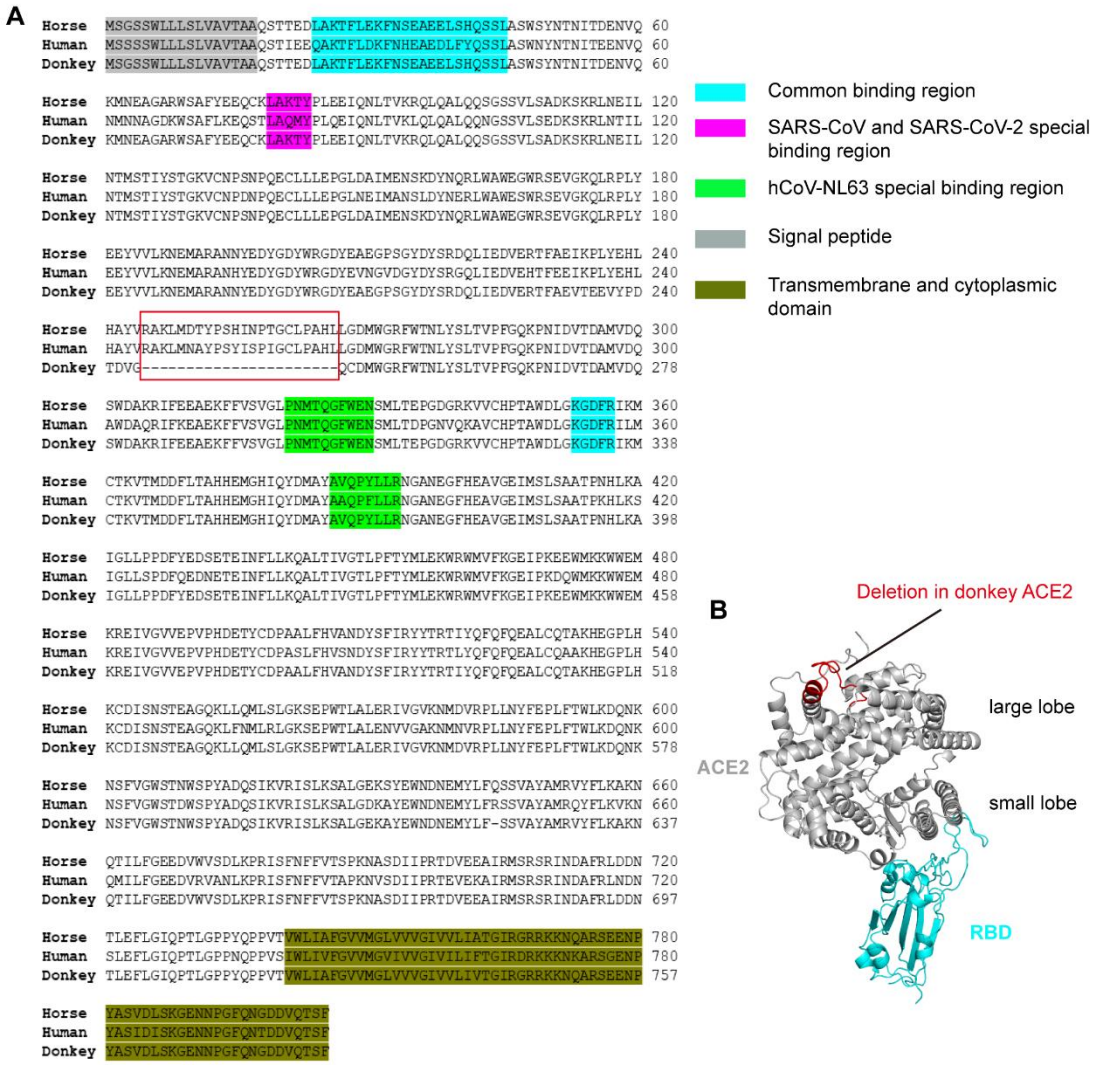

Supplementary Figure 2 Sequence alignment of ACE2 orthologs, related to Figure 2. (**A**) Horse, human and donkey ACE2 orthologs were aligned and the predicted binding regions of ACE2 recognized by the RBDs of the three ACE2-dependent coronaviruses were highlighted with different colors. Residues in cyan and magenta were predicted to bind to SARS-CoV and SARS-CoV-2; residues in cyan and green were predicted to bind to hCoV-NL63. The signal peptide was shown in grey, while the transmembrane and cytoplasmic domains were colored in palm green. (**B**) The deletion in donkey ACE2 is labeled.

Supplementary Table 3 Summary of SARS-CoV-2 variants, related to Figure 4.

WHO label	WHO definition	Pango lineages	Earliest documented samples	Mutations		
				NTD	RBD	others
Alpha	VOC	B.1.1.7	United Kingdom	69-70del, Y144del	N501Y	A570D, D614G, P681H, T716I, S982A, D1118H
Beta	VOC	B.1.351	South Africa	D80A, D215G, 242-244del	K417N, E484K, N501Y	D614G, A701V
Gamma	VOC	P.1	Brazil	L18F, T20N, P26S, D138Y, R190S	K417T, E484K, N501Y	D614G, H655Y, T1027I, V1176F
Delta	VOC	B.1.617.2	India	T19R, G142D, 156-157del, R158G, A222V	L452R, T478K	D614G, P681R, D950N
Omicron	VOC	B.1.1.529	South Africa and Botswana	A67V, 69/70del,T95I,DEL142/144,Y145D, Δ211/L212I, ins214EPE	G339D,S371L,S373P,S375F,K417N,N440K, G446S,S477N,T478K,E484A,Q493R,G496S, Q498R,N501Y,Y505H	T547K,G614D,H655Y,N679K,P681H,N764K,D769Y, N856K,Q954H,N969K,L981F
Kappa	VOI	B.1.617.1	India	T95I, G142D, E154L	L452R, E484Q	D614G, P681R, N1071H
n/a	VOI	A23.1	Uganda/Liverpool	F157L	V367F	Q613H, P681R
Eta	VOI	B.1.525	Nigeria (Multiple countries)	Q52R, A67V, 69-70del, Y144del	E484K	D614G, Q677H, F888L
Epsilon	VOI	B.1.429	US, CA	S13I, W152C	L452R	D614G
Iota	VOI	B.1.526	US, NY	L5F, T95I, D253G	E484K	D614G, A701V

Lambda	VOI	C.37	Peru	G75V,T75I,R246N,DEL247/353	L452Q,F490S	D614G,T859N
Mu	VOI	B.1.621	Colombia	T95I,Y144S,Y145N,	R346K,E484K, N501Y	D614G,P681H,D950N
Delta plus	VUM	B.1.617.2 + K417N	United Kingdom	T19R, G142D, 156-157del, R158G, A222V	K417N，L452R, T478K	D614G, P681R, D950N

n/a: not applicable, no WHO label has been assigned to this variant at this time.

Supplementary Figure 3

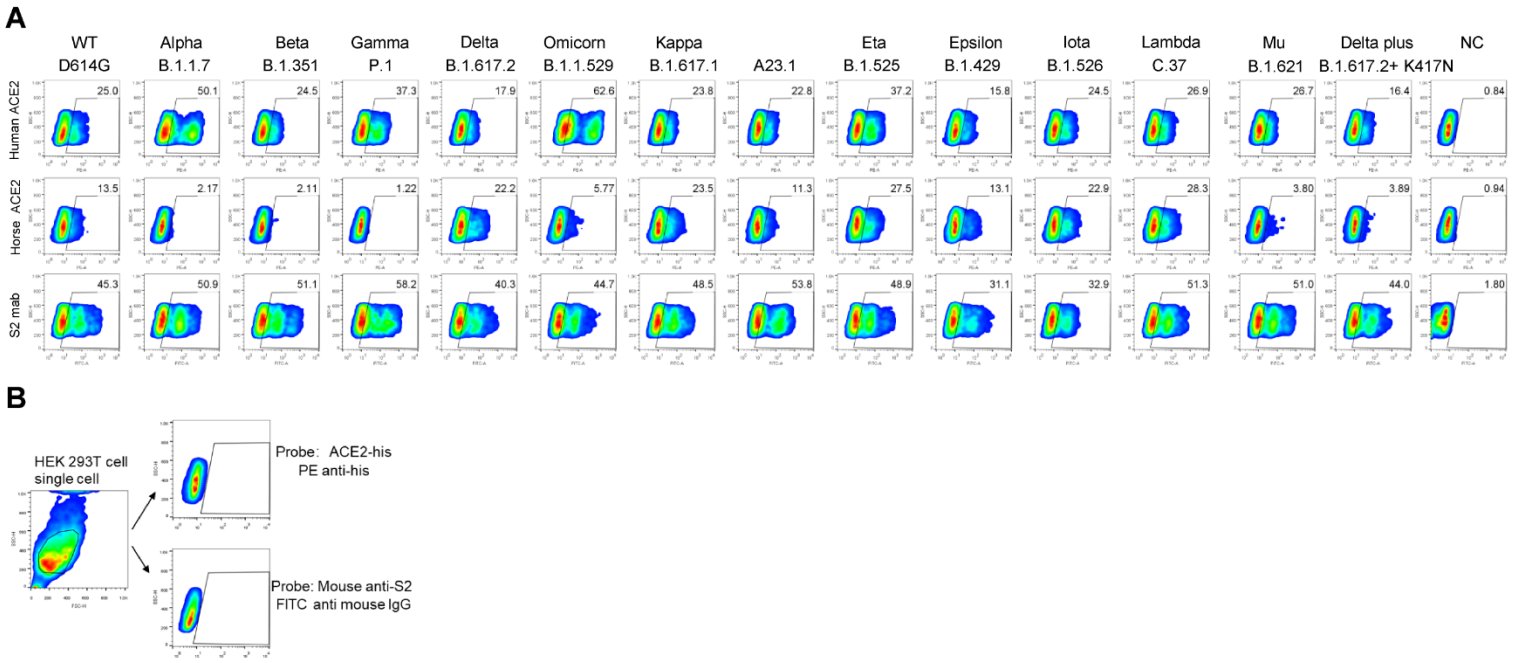

Supplementary Figure 3 Binding of HEK 293T cell surface expressed SARS-CoV-2 variants by eACE2 and hACE2, related to Figure 4. Wildtype D614G and mutant S proteins were expressed on the surface of HEK 293T cells, incubated with the eACE2 or hACE2, followed by staining with PE anti-his or FITC anti-mouse IgG, and analyzed by FACS. The percentage of positive cells is shown in the gate. S2 is used as a positive control for normalization of S expression. NC (negative control) contained mock-transfected HEK 293T cells. Data shown were taken from one of two independent experiments.

Supplementary Figure 4

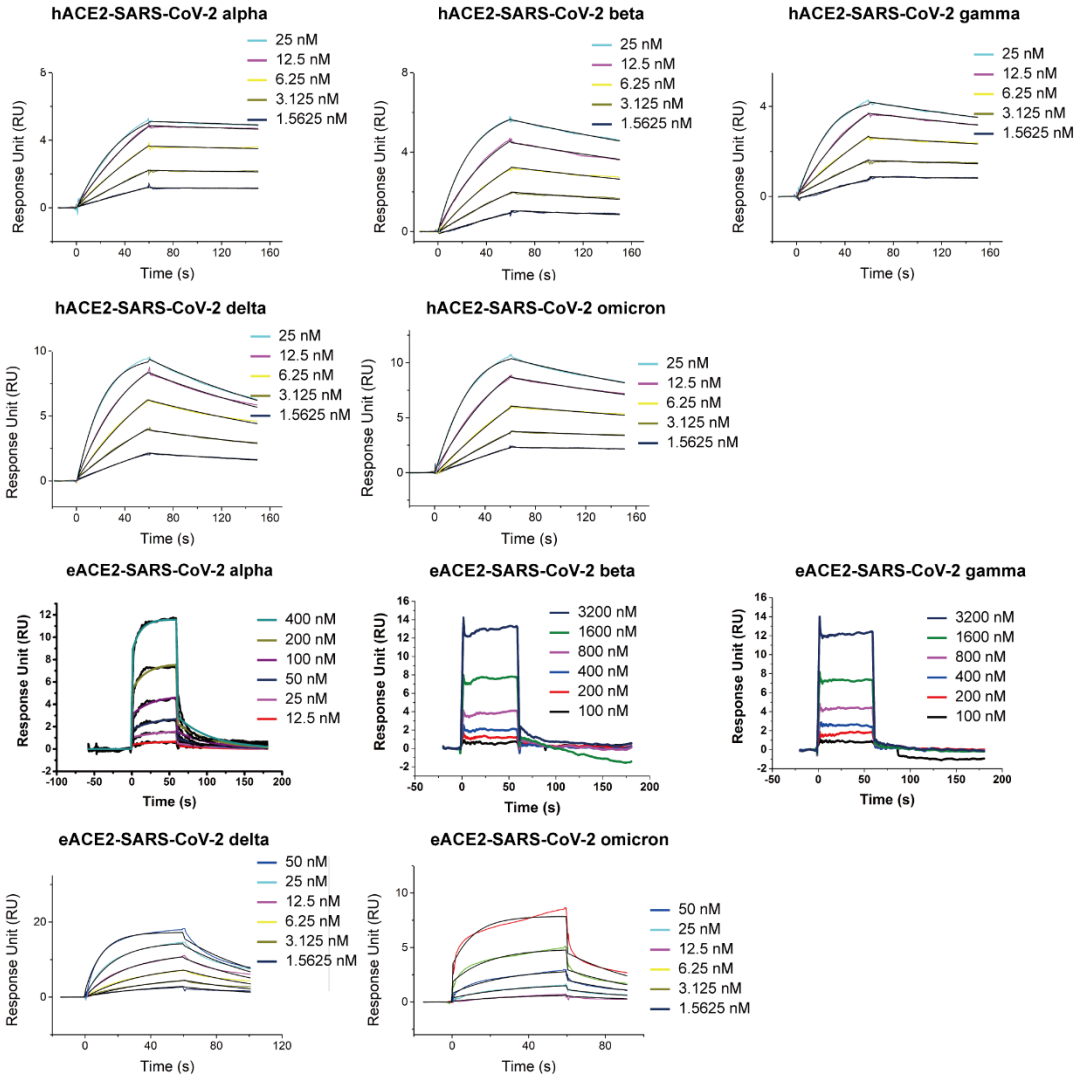

Supplementary Figure 4 The binding of equine and human ACE2 orthologs with RBDs of SARS-CoV-2 variants, related to Figure 4. (**A**) SPR characterizations of the binding between eACE2 or hACE2 and RBD of SARS-CoV-2 variants. eACE2 or hACE2 was immobilized on the CM5 chip and RBDs were flowed through. The raw and fitted curves were displayed in colored and black lines, respectively.